Hindawi Publishing Corporation
EURASIP Journal on Image and Video Processing
Volume 2010, Article ID 524613, 13 pages
doi:10.1155/2010/524613

Research Article

Rate Control Performance under End-User's Perspective: A Test Tool

Cristian Koliver,[1] Jean-Marie Farines,[2] Barbara Busse,[3] and Hermann De Meer[3]

[1] *Center for Computing and Information Technology, University of Caxias do Sul, P.O. Box 1352, Caxias do Sul, Brazil*
[2] *Department of Automation and Systems Engineering, Federal University of Santa Catarina, P.O. Box 476, Florianopolis, Brazil*
[3] *Department of Mathematics and Computer Science, University of Passau, Innstrae 43, 94032 Passau, Germany*

Correspondence should be addressed to Cristian Koliver, ckoliver@ucs.br

Received 30 April 2009; Revised 9 November 2009; Accepted 19 January 2010

Academic Editor: Benoit Huet

Copyright © 2010 Cristian Koliver et al. This is an open access article distributed under the Creative Commons Attribution License, which permits unrestricted use, distribution, and reproduction in any medium, provided the original work is properly cited.

The Internet has been experiencing a large growth of multimedia traffic of applications performing over an RTP stack implemented on top of UDP/IP. Since UDP does not offer a congestion control mechanism (unlike TCP), studies on the rate control schemes have been increasingly done. Usually, new proposals are evaluated, by simulation, in terms of criteria such as fairness towards competing TCP connections and packet losses. However, results related to other performance aspects—quality achieved, overhead introduced by the control, and actual throughput after stream adaptation—are difficult to obtain by simulation. In order to provide actual results about these criteria, we developed a comprehensive live video delivery tool for testing RTP-based controllers. In this version of the tool, the video is encoded on the fly in the MPEG-2 standard, but we intend to use the H.264/AVC standard as soon as common PC's provide enough processing power to encode H.264/AVC live video. The tool allows to easily incorporate new control schemes. In this paper, we describe the tool architecture and some implementation details. We also evaluate the performance of the tool itself, in terms of efficacy, accuracy, and efficiency.

1. Introduction and Motivation

Many end-to-end rate control strategies for real-time multimedia applications have been proposed in the last years. Most of them are driven to UDP applications running over the best effort Internet. They are control systems-like, on which the server adapts its throughput based on feedback messages from the clients. The messages are sent in short intervals. The goals of the rate control strategies include to avoid network congestion and provide TCP-friendliness [1]. Since the RTP (Real-time Transport Protocol) was designed by the IETF (Internet Engineering Tasking Force) for multimedia communication in the Internet and offers support for collecting information about network load, packet losses and end-to-end delays, the strategies are usually based upon this protocol (see, e.g., [2, 3]).

Pawlikowski shows in [4] the results of a survey of over 2246 research papers on the network published in the IEEE journals and conferences. The survey revealed that over 51% of all publications on the network adopt computer simulation to verify their ideas and report network performance results. As mentioned by Ke et al. in [5], when evaluating video delivered quality, most of previous studies adopt a video trace file as video stream source in their simulation environment. The advantage is simplicity because researchers do not know much about the concept of video encoding and decoding. But, in the same time, the researchers could not dynamically change the video encoding parameters because of the same reason. In addition, simulations do not provide results related to performance criteria such as the quality oscillation and the overhead introduced by the controller and the actuator. In this paper, we describe a modular live video delivery tool designed for testing RTP-based rate controllers. It allows to easily incorporate new rate control schemes. We also show the results that the tool can provide and evaluate its performance in terms of efficacy and efficiency.

The paper is organized as follows. The architecture of the tool is presented in Section 2. In Section 3, we provide implementation details of the tool. We investigate the performance of our tool in Section 4. In Section 5, we review some related work. Finally, in Section 6, we discuss the results and further work to improve the tool.

2. Architecture

Figure 1 depicts the architecture of our video delivery tool. In this figure, there is a single client but the server may multicast the video stream to m clients. At the server-side, the tool is formed of four separated modules: the MPEG-2 encoder, the packetizer, the controller, and the actuator.

The encoder compresses the raw video stream (from now designated as *test video*) on the fly and has N QoS parameters ρ_p $(p = 1, 2, 3, \dots, N)$ to be set. They have influence on the stream bit rate (by affecting the compression rate) and quality. A combination of QoS parameters settings is a QoS level. The kth QoS level L_k is an N-tuple

$$L_k = \langle \rho_{1_k}, \rho_{2_k}, \dots, \rho_{N_k} \rangle, \tag{1}$$

where $k = 1, 2, \dots, I$ (I is the module of the Cartesian product of the QoS parameters domains). When the encoder is set as L_k, the *expected* stream bit rate is rn_k (the *nominal rate*) and the quality is qn_k (the *nominal quality*). This latter metric should reflect the stream quality according to the user perspective. In our tool, it is used to rank QoS levels (see details in Section 3.1).

The packetizer assembles the MPEG-2 video stream provided by the encoder in RTP packets and delivers them over the network. At the client-side, there are two modules: the depacketizer and the MPEG-2 decoder. The depacketizer converts RTP packets into MPEG-2 elementary streams and provides a feedback to the packetizer through receive report (RR) packets. The packetizer computes and provides the controller with losses (l) and round trip delay (τ). In the adaptation instant t, the controller computes the *target rate* $rt(t)$ providing it to the actuator.

The actuator uses the function $\mathcal{Q}oS$ to find a QoS level L_k whose rn_k matches $rt(t)$. The function is

$$\mathcal{Q}oS : rt(t) \longmapsto \langle L_k, rn_k, qn_k \rangle, \quad rn_k \leq rt(t). \tag{2}$$

The function $\mathcal{Q}oS$ is built from a video designated here as *reference video*. The reference video should be of the same kind (but not the same video) as the test video. We should at least have three different $\mathcal{Q}oS$ functions: one built from an action video, a second one built from a talking head video, and a third one built from a cartoon video (Different kinds of video contents affect the compression rate and, consequently, the stream bit rate. The perceived quality of the video is also affected by the video content.). We suggest these three types of videos to build three different $\mathcal{Q}oS$ functions based on the video quality test method proposed in ITU-R BS.116-1 Recommendation, the double-blind triple-stimulus with hidden reference. The division according to the video content into action video, talking head video, and cartoon video is due to that an action video usually contains much larger movement than a talking head video. Hence, viewers may easier perceive the jerky motion with the loss of frames in action video. Cartoons videos, in turn, allow sudden changes in motion, because users generally expect artificial movements in this type of video. Then, the actuator adjusts the encoder parameters

$$\rho_1, \rho_2, \dots, \rho_N \tag{3}$$

to $\langle \rho_{1_k}, \rho_{2_k}, \dots, \rho_{N_k} \rangle$. The configuration of the encoder after adapting is $L(t) = L_k$. Each adaptation instant $t+1$, the actuator measures the encoder throughput between $t-1$ and t (the *actual rate* achieved after adaption instant $t-1$ or $ra(t-1)$) as well as $qa(t-1)$ (the quality actually achieved after adapting). These values are provided to the actuator to tune $\mathcal{Q}oS$. Note that it is expected that $ra(t-1) \approx rt(t-1) \approx rn_j$ and $qa(t-1) \approx qn_j$ $(L_j = L(t-1))$.

During the transmission, the tool collects and stores several data that will permit a rate controller performance analysis, such as: output frame rate, losses, bit rate, and quality variation, at the server side, and frame rate, at the client side.

3. Implementation

In this section, we provide the main implementation details of each module, since some of the achieved results are closely related to the tool design aspects. Furthermore, some ideas used here may be useful for other rate controllers implementations.

3.1. The Controller.

The controller can be viewed as a black box whose inputs are the round trip delay and the loss rate and the output is the target throughput. It is implemented as a periodic task whose period is P. Period P is the feedback period defined by the RTP.

A rate controller may compute $rt(t)$ values slightly different from $rt(t-1)$ values (less than 50 Kbps), generating thus highly granular target bit rates. Therefore, practical use of rate controller driven to multimedia applications requires a strategy to configure the application in order to achieve a throughput similar to the target throughput $rt(t)$ computed by the controller. In our tool, the strategy is implemented by the actuator, described in the next section.

3.1.1. The Actuator.

The actuator is responsible for configuring the encoder parameters as L_k in time t, such that rn_k is close (but not greater) to the target throughput $rt(t)$ provided by the controller.

Since the controller can generate values of the target bit rates differing by some few Kbps, our main concern in the actuator design was to define a strategy for providing fine granularity in terms of rn_k and qn_k values. Common strategies of actuation focusing on a single quality dimension (e.g., strategies based on frame dropping or quantizer adjustment) are unsuitable, since they provide a very discrete set of bit rates values. The application user perceives such limitation as sudden changes of quality; under the network point of view, the mapping from $rt(t)$ into a QoS level L_k possibly leads to the bandwidth underutilization. Thus, we opted to use N dimensional QoS levels composed by the following parameters: alternate scan (als), prediction type (mtc), quantization

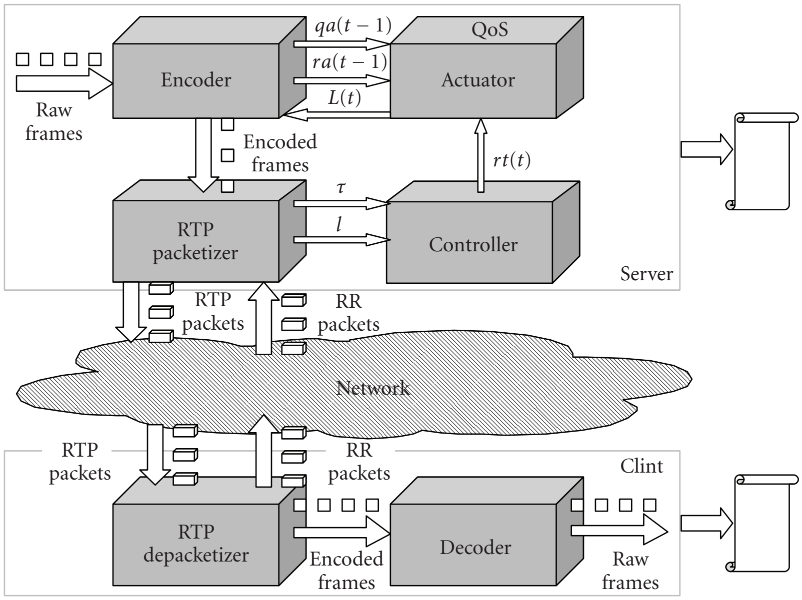

Figure 1: Video delivery tool architecture.

factor or quantizer (qtz), intra-inter matrix combination (mqt), DC precision (dcp), and matrix of coefficients (mcf) (see http://www.mpeg.org/MSSG/tm5/index.html for more details about purpose and influence of these parameters on the compression process). We run several tests using different set of parameters. The above one was chosen by providing a fine quality/rate granularity.

The actuator selects the QoS level L_k from a table denoted by $\mathcal{Q}oS_T$. $\mathcal{Q}oS_T$ is a table whose entries are tuples as

$$\langle \langle als_k, mtc_k, mqt_k, qtz_k, dcp_k, mcf_k \rangle, rn_k, qn_k \rangle, \quad (4)$$

where als_k is the value of parameter als in the k th table entry, mtc_k is the value of parameter mtc, and so on; rn_k is the nominal throughput of the encoded video stream configured as L_k; and qn_k is the nominal quality of this stream given by the average of the signal-to-noise ratio (SNR). Indeed, $\mathcal{Q}oS_T$ represents $\mathcal{Q}oS$ and it is an extension of the degradation path strategy [6–8], an ordered list of available QoS levels and encodings and their resource requirements (particularly, bandwidth). The list is limited by user's choices and by hardware constraints. The degradation path varies according to what the users trade offs are.

3.1.2. Construction of $\mathcal{Q}oS_T$. $\mathcal{Q}oS_T$ is automatically built once for a given server prior to the transmission (note that different power processing servers may generate different values of rn_k). The $\mathcal{Q}oS_T$ construction is an iterative process, where the same short raw clip (the reference video) is compressed again and again setting the encoder parameters, in each iteration k, as L_k. For each iteration k, the variables rn_k and qn_k are computed. Then, the tuple given by (4) is stored as a $\mathcal{Q}oS_T$ entry. $\mathcal{Q}oS_T$ is stored in a file (referenced as $\mathcal{Q}oS_T$ file), to be used for different live video transmissions. When a video transmission is started, the file is loaded in the multilist. Figure 2 shows a same frame of the reference video, used to build $\mathcal{Q}oS_T$ for our tests, compressed with the QoS levels L_i (Figure 2(a)) and L_j (Figure 2(b)). Note that whereas $rn_i \approx rn_j$, qn_i and qn_j are very different.

The $\mathcal{Q}oS_T$ magnitude may introduce a non-trivial overhead when seeking a QoS level L_k such that $rn_k \approx rt(t)$. In order to reduce this delay, $\mathcal{Q}oS_T$ is represented internally like a multilist whose first level nodes represent throughput subranges. Thus, the complexity of seeking is reduced to the number of subranges rather than the number of QoS levels. We defined the actuator granularity as 25 Kbps steps and 10,000 Kbps as the maximum nominal throughput. The granularity is a constant easily changeable. However, we believe that lower values improve granularity but, on the other hand, they degrade accuracy. Therefore, node 0 represents the throughput subrange $[0; 25[$ Kbps; node 1 represents $[25; 50[$; node Π represents the throughput subrange $[\Pi \times 25; (\Pi+1) \times 25[$; the 401st node represents the subrange $[10000; \infty[$. Each first level node Π has associated a second level list (sublist) whose π nodes contain tuples $\langle \langle als_i, mtc_i, mqt_i, qtz_i, dcp_i, mcf_i \rangle, qn_i \rangle$ $(i = 1, 2, \ldots, \pi)$. The value rn_π is not stored but it follows the property

$$rn_\pi \in [\Pi \times 25; (\Pi + 1) \times 25[. \quad (5)$$

Sublists are sorted in descendant order by qn. Figure 3 shows the multilist structure. Some first level list nodes may contain an empty sublist; most of the sublists contain thousands of nodes. During transmission, $\mathcal{Q}oS_T$ adjusts itself to the video which is currently transmitted: at the adaptation instant t, the quality qn_k and the throughput rn_k of the current QoS level $L_k = L(t-1)$ are recomputed ($qn_k \leftarrow qa(t-1)$ and $rn_k \leftarrow ra(t-1)$). As a result, a head node of a sublist can change its position within its sublist or even move to another sublist. Then, the sublist heads are not static (the reason for keeping the sublists rather than only the heads).

(a) (b)

Figure 2: Same frame of the reference video when the stream QoS levels are: (a) $\langle\langle 1, 4, 62, 2, 8, 2\rangle, 1047.86, 8.96\rangle$ and (b) $\langle\langle 6, 6, 10, 4, 8, 2\rangle, 1045.09, 21.80\rangle$.

When using the tool for delivering a test video, the actuator runs concurrently with the controller and performs only after the end of a GOP because to change some parameters during a GOP processing may cause side-effects (e.g., runtime errors due to absence of enough structures to store macroblocks, since the number of structures allocated depends on the GOP pattern and if they are allocated at the beginning of the GOP processing). Therefore, the actuation period varies according to the GOP time processing and it is often much shorter than the control period, that is, while the controller does not compute $rt(t)$, the actuator goes on adapting the encoder bit rate to $rt(t-1)$. From one standpoint, the actuator works unnecessarily. By using a fine-grained period, however, the actuator constantly tailors the multilist representing the $\mathcal{Q}oS_T$ table to the test video content, improving the tool accuracy.

3.1.3. Actuation Steps. Let L_i be the current QoS level at instant $t-1$ (i.e., $L(t-1) = L_i$). In adaptation instant t, the actuator receives the estimated $rt(t)$ value from the controller and performs the following steps:

(1) seeks a node π such that $rt(t) \geq (\pi + 1) \times 25$ and whose sublist head is the QoS level L_j of highest qn_j;

(2) sets the encoder as L_j (now, L_j is the current QoS level);

(3) updates the nominal throughput and quality values of L_i ($rn_i \leftarrow ra(t-1)$ and $qn_i \leftarrow qa(t-1)$).

For example, let $L(t-1) = L_i = \langle 0, 6, 2, 4, 0, 0\rangle$ be the current QoS level of the stream (see Figure 3(a)); the current nominal throughput $rn(t-1)$ is a value between $[8525; 8550[$ Kbps and the current nominal quality $qn(t-1) = qn_i$ is 30.2154. Let us suppose that at the adaptation instant t, the controller computes $rt(t) = 8612.80$. In this case, the actuator:.

(1) seeks, among the first level nodes, that one whose upper limit of subrange is less or equal to 8612.80 (then, the search goes until the subrange $[8600; 8625[$). The selected QoS level is that one with the highest nominal quality whose node is the sublist head of the subrange $[8600; 8625[$ ($L_j = \langle 0, 3, 2, 3, 8, 1\rangle$ and $qn_j = 30.9252$; Figure 3(b));

(2) sets the encoder as L_j (Figure 3(c));

(3) letting 7851.4567 Kbps and 30.2001 dB be, respectively, the throughput and the quality measured by the actuator between $t-1$ and t (we mean, $ra(t-1)$ and $qa(t-1)$), then it updates rn_i to 7851.4567 and qn_i to 30.2001. This implies in relocating L_i to the subrange $[7850; 7875[$.

3.2. Encoder. The encoder is a modified version of the University of Berkeley's encoder, which follows the test model 5 (TM5). Since its source code is freely distributed and reasonably well documented, this encoder has been used for educational purposes and as reference for other implementations. We chose an MPEG-1/2 encoder rather than H.264/AVC (more suitable for compression on the fly) due to the simplicity of Berkeley's encoder code, what makes it easily modifiable. Furthermore, H.264/AVC encoders implemented by software have a very high CPU demand, a critical feature for applications with latency and real time response requirements. The demand is due to the high computational complexity of motion estimation, because of the serial coding nature and high data dependency of coding procedure in both CAVLC and CABAC. When the H.264/AVC encoder use is combined with high resolution video, the only adequate platforms are those with supercomputing capabilities (e.g., clusters, multiprocessors and special purpose devices) [9]. However, the other modules of the tool are reasonably (but not totally) independent from the encoder. Thus, the replacement of the MPEG-1/2 encoder in the tool by another would not be a so hard process (we describe the main actions required in Section 6).

Originally, the encoder input is a parameter configuration (*.par*) file with the encoder configuration (resolution, frame rate, quantization matrices, and so on) and the raw video file name to be compressed; the output is a file containing a MPEG-1/2 stream. We modified the Berkeley's encoder so that it supports: (1) *variable bit rate (VBR) stream generation:* originally, the encoder generates CBR

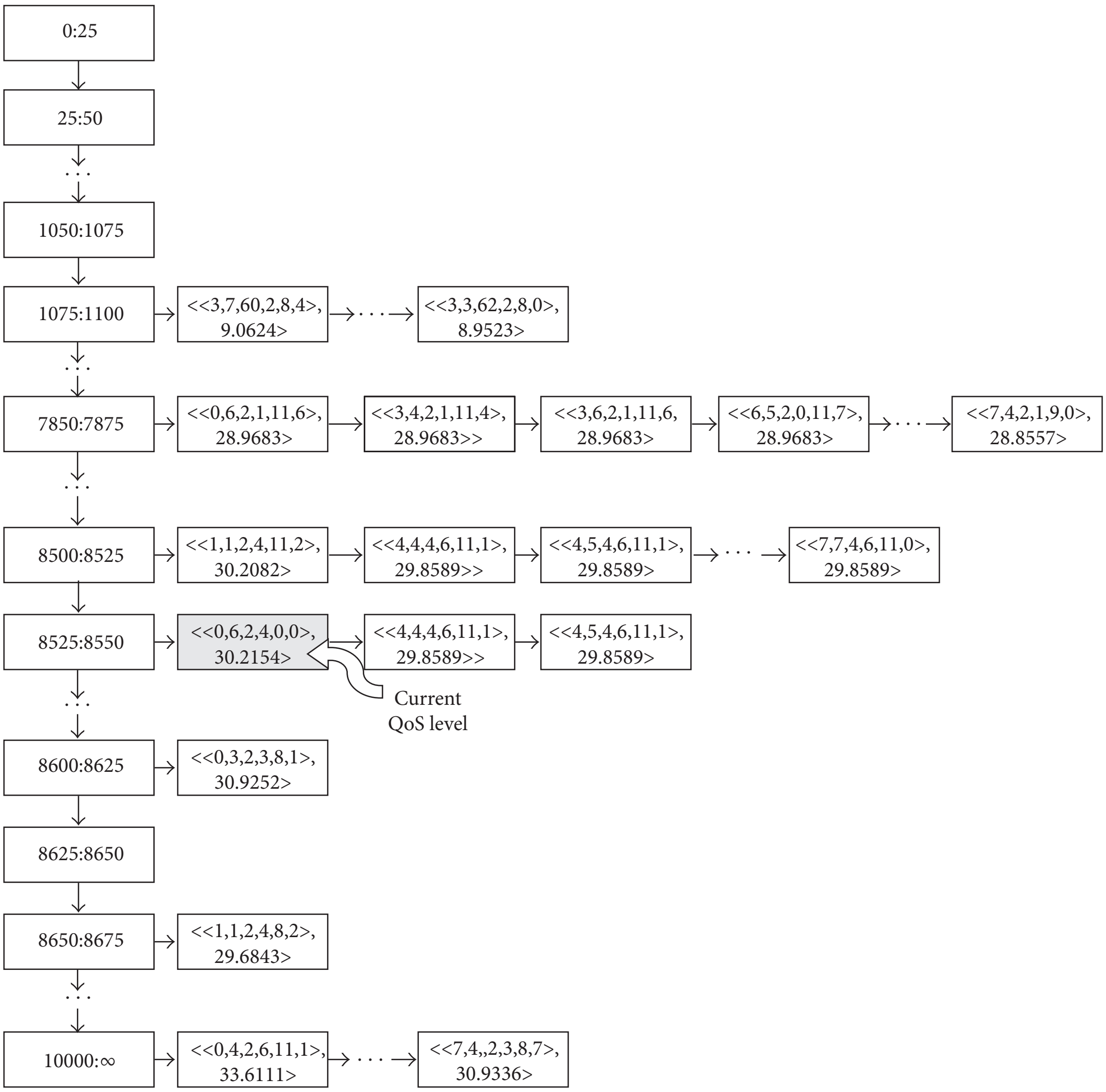

(a)

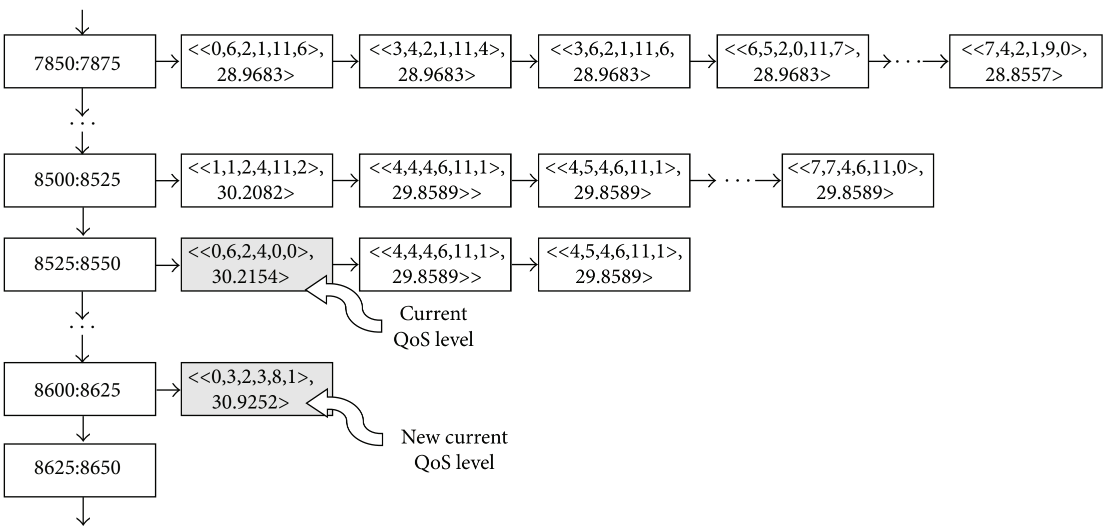

(b)

Figure 3: Continued.

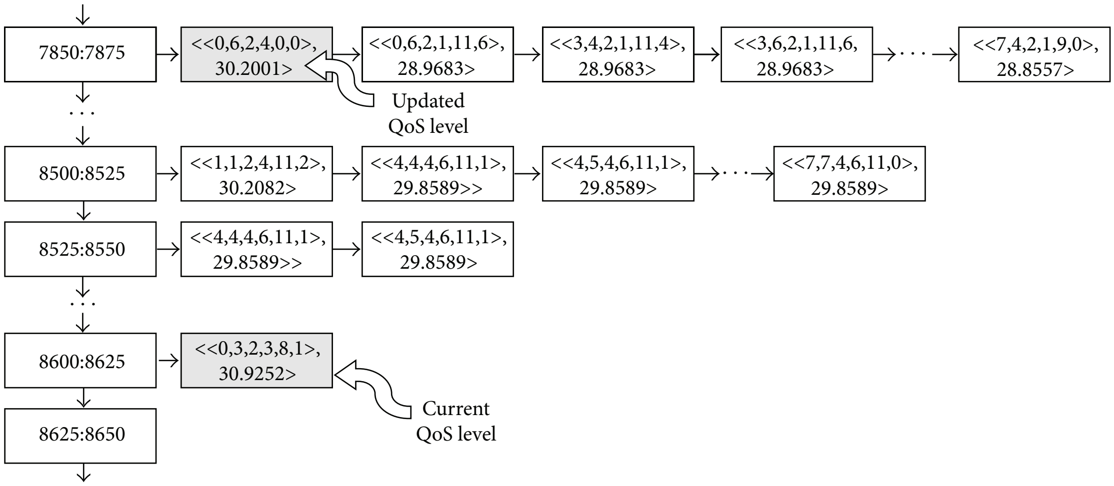

(c)

Figure 3: Self-adjustment mechanism of the multilist representing $\mathcal{Q}oS$.

streams whose target throughput is specified in the *par* file. This throughput is achieved adjusting, during the compression process, the quantizer value. Our version generates a VBR stream, since the target throughput generated by the controller is variable; (2) *stream transmission:* the original encoder/decoder are independent programs whose inputs and outputs are files. Our version follows the client-server model. The server begins the transmission to a host (the client) or to a multicast address; (3) *command line configuration:* the *par* file is not used anymore; the encoder configuration can be done by command line. This modification is needed to automatically generate the $\mathcal{Q}oS_T$ table (afterwards, the configuration is not necessary anymore since the encoder settings change dynamically during video compression/transmission); (4) *mean signal-to-noise ratio computation:* originally, Berkeley encoder computes SNR for each component Y, U and V of each frame (Y represents the luminance or luma component of a pixel, U and V the color difference components or chroma.). Now, it computes the mean SNR ($\overline{\text{SNR}}$) between frames i and $i+k$ ($k \in \mathbb{N}^*$) according to the following equation:

$$\overline{\text{SNR}} = \frac{\sum_{j=i}^{i+k} \text{SNR}_Y(j) + \text{SNR}_U(j) + \text{SNR}_V(j)}{k+1}, \qquad (6)$$

where j is the j th sample (frame), and $\text{SNR}_Y(j)$, $\text{SNR}_U(j)$ and $\text{SNR}_V(j)$ are the SNR values of the frame components Y, U, and V ($\overline{\text{SNR}}(L_i) = qn_i$); and (**5**) **mean throughput computation:** the encoder now computes the throughput between frames j and $j+k$. This computation is needed for the creation and the self-adjustment mechanism of $\mathcal{Q}oS_T$.

3.3. SNR as a Quality Measure. Measuring quality is not always a straightforward process due to the subjective nature of quality. Usually, video quality is evaluated through two different approaches: objective and subjective tests.

The objective tests usually do not take the human perception of the quality into account in their results. It is well known that the metric used for assessing video quality in our work—SNR—and the peak signal-to-noise ratio (PSNR) are not correlated with human visual system (HVS). A problem of these metrics, based on the mean square error (MSE) computation, is that even though two images may be different, the visibility of this difference is not considered. They do not take into consideration any details of the HVS such as its ability to "mask" errors that are not significant to the human comprehension of the image. Cranley et al. [10] provide an example of this problem. Consider an image where the pixel values have been altered slightly over the entire image and another image where a small part of the image concentrates all alterations. Both may have the same MSE value, but they appear to be very different to the user.

In addition, SNR does not effectively predict subjective responses for MPEG video systems. In tests performed by Nemethova et al. [11], SNR captured only about 21% of the subjective information that could be captured considering the level of measurement error present in the subjective and objective data.

On the other hand, there is not a consensus about the accuracy of the results provided by traditional video tests methodologies when used for assessing quality for multimedia applications. Watson and Sasse, for example, argue in [12] that ITU-recommended methods for subjective quality assessment of speech and video are not suitable, among other reasons, because:

(1) the 5-point quality scales are not viable due to their vocabulary: it is expected the responses to be biased towards the bottom of the scale. The DSCQS permits scoring between the categories (the subject places a mark anywhere on the rating line, which is then translated into a score), but it is still the case that subjects shy away from using the high-end of the scale and will often place ratings on the boundary of the "good" and "excellent" ratings;

(2) there is no particular reason for using five scales;

(3) the quality tests typically require the viewer to watch short sequences of approximately 10 seconds in duration, and then rate this material. It is not clear that a 10-second video sequence is long enough to experience the types of degradations common to multimedia applications;

(4) the quality judgments are intended to be made entirely on the basis of the picture quality. It should be queried whether it makes sense to assess video on its own (i.e., without audio), since it would be true to say that the video image in a multimedia application does not have the same importance as in the television system;

(5) results based on the difference between the degraded sequence and the reference used for subjective quality evaluation can differ significantly in some cases according to the test method, thus also providing limited means for the appropriate quality estimation; and

(6) "one-off" quality ratings gathered at the end of an audiovisual session do not capture change of perceptions about the quality that users may have during communication across a packet network with varying conditions.

In our tool, even newer and more suitable testing methodology, driven to quantify multimedia applications quality, are not viable, due to the hundreds of QoS levels used by the $\mathcal{Q}oS$ function. An alternative to SNR or PSNR to rank the quality is the video quality metric (VQM) from National Telecommunications and Information Administration (NTIA, http://www.its.bldrdoc.gov/vqm/), a standardized method of objectively measuring video quality that, according to the ITU-T [13], closely predicts the subjective quality ratings that would be obtained from a panel of human viewers. The VQM has the advantage of consisting of a set of objective metrics, each designed for a different target application.

4. Tool Performance Analysis

Our tool provides data which allow to evaluate the performance of the rate controller in terms of reduction of losses, smoothness of throughput change, adaptation overhead, and, mainly, video quality achieved. In this section, however, we describe results that permit to evaluate the performance of the tool itself. We used, just as a case-study, a controller following the Enhanced Loss-Delay Algorithm (LDA+), proposed by Sisalem and Wolisz [14]. The LDA+ controller regulates the server throughput based on end-to-end feedback information about losses, delays and the bandwidth capacity measured by the m clients. This information is sent by the clients to the server in the RR packets of RTCP protocol. The LDA+ controller uses additive increase and multiplicative decrease factors determined dynamically at the server-side to compute $rt(t)$. The factors come from an estimative of the current network status from the above information (see [14] for more details about $rt(t)$ computation). Note that *any* rate controller whose inputs and outputs are those showed in Figure 1 could be used to get the data to evaluate the tool performance.

The tool performance is evaluated in terms of its efficacy, accuracy and efficiency.

4.1. Efficacy and Efficiency Aspects. A tool for testing rate controllers should have a mechanism that efficaciously maps the target bit rate into QoS application parameters, such as the application bit rate matches or is close to the target bit rate. In order to check if our tool reaches this goal, we measure the error $\epsilon(rt(t), ra(t))$, the difference between the target bit rate and the bit rate actually achieved.

Another aspect related to the tool efficacy is the achieved quality. Quality should follow bit rate, that is, the higher bit rate, the higher quality. If quality does not follow bit rate, then the actuator is not selecting the best QoS level for a given target bit rate. In order to evaluate this relationship, we analyze the behavior of $qa(t)$ compared to $ra(t)$.

In terms of the tool accuracy, we analyze the errors $\epsilon(rt(t), rn(t))$ and $\epsilon(rn(t), ra(t))$. Large values of the first one—the difference between the target bit rate computed by the controller and the bit rate selected in the $\mathcal{Q}oS_T$ table by the actuator—indicate that $\mathcal{Q}oS_T$ is too coarse. Even if we have thousands of QoS levels, the set of really useful QoS levels may be short, since many of them offer the same quality and/or bit rate. Thus, the granularity *de facto* can be known just after generating the multilist representing $\mathcal{Q}oS_T$, regardless the actuator granularity (25 Kbps; see Section 3.1). A coarse $\mathcal{Q}oS_T$ implies sudden changes of quality, even if the controller gradually changes the allowed bit rate.

The error $\epsilon(rn(t), ra(t))$—the difference between the nominal bit rate and the bit rate actually achieved—is due to the differences between the reference and test videos. The scene content influences the compression rates obtained in the temporal and spatial redundancy steps. Therefore, encoded frames of the reference and test videos may present different compression rates even if they are set to the same QoS level. Large $\epsilon(rn(t), ra(t))$ values indicate that the bit rate values of $\mathcal{Q}oS_T$ (rn_k) are excessively related to the reference video. We expect that this error tends to lower during the transmission, due to the self-adjusting mechanism of $\mathcal{Q}oS_T$.

Two important aspects related to the tool efficiency are CPU and memory consumption. Since the encoding process has a high CPU and memory usage rate, other tool modules (controller, actuator, and RTP packetizer) should consume a minimum of such resources. Otherwise, it can introduce an overhead in the encoding process increasing the end-to-end delay. In our tool, the most critical data structure in terms of memory requirements is the multilist representing $\mathcal{Q}oS_T$. Therefore, our focus here is to analyze if it is possible to reduce its size. For evaluating the overhead introduced by the tool, we compare the response time of the actuator after receiving $rt(t)$ from the controller, since the most time-consuming module of the tool—excepting the encoder—is the actuator. (Note that the very high cost process of building the $\mathcal{Q}oS_T$ file is performed once and prior to

Figure 4: Video used in the tests.

the transmission. Furthermore, the same QoS_T file can be used for different video transmissions).

4.2. Test Environment. In order to evaluate the capabilities of the proposed tool, we conducted a set of transmissions to investigate its performance and to show the data provided by it.

The transmissions were performed using a server host connected to a client host via a router host configured with the RED algorithm to drop packets whenever congestion arises in the network. The physically available bandwidth among the hosts was 100 Mbps, but the server-client link bandwidth was restricted to 6 Mbps, in order to represent a network bottleneck. The reference video used to construct QoS_T was a talking heads slow motion clip (the News clip, see Figure 2). The test video was the Salesman clip (see Figure 4) (both videos are raw video sequences in the YUV QCIF format publicly available for downloading at http://trace.eas.asu.edu/yuv/) The feedback period is 5 seconds (the RTCP sending interval used by Sisalem and Woliz in the LDA+ tests).

4.3. Results. Figure 5 shows a histogram representing the QoS levels distribution of QoS_T for a server with two hyper-Threading Intel Xeon 2.80 GHz processors. Note that subranges between 1075 and 5000 Kbps concentrate most of the QoS levels. The subranges below 200 Kbps do not have any QoS levels (sublists) associated (and there are some gaps between 200 and 750 Kbps). Therefore, the actuator has to map the target rates below 200 Kbps into the QoS level L_k such as $rn_k = 200$ Kbps. In a rate controller of a practical application, this gap could be filled by buffering (e.g., introducing a delay). Indeed, it is possible to reduce or increase the server throughput through buffering, regardless the QoS level likely CBR applications. However, this approach can lead to an unacceptable end-to-end delay for live video applications.

Figure 6 shows the behavior of $rt(t)$, $rn(t)$ and $ra(t)$. Note that the behavior of the curve rn is close to the behavior of the curve rt. In fact, these variables are strongly correlated: the correlation coefficient obtained was 0.949 and the P-value is.0.

The harmonic mean of the absolute values of the errors $\epsilon(rt(t), rn(t))$ is 55.2688 Kbps, a not so large value. As showed in Figure 7, from time 0 to about 300, the error

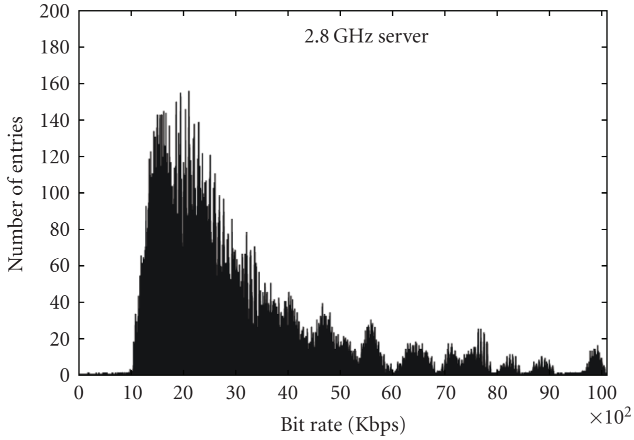

Figure 5: QoS levels distribution per throughput subranges (fast server).

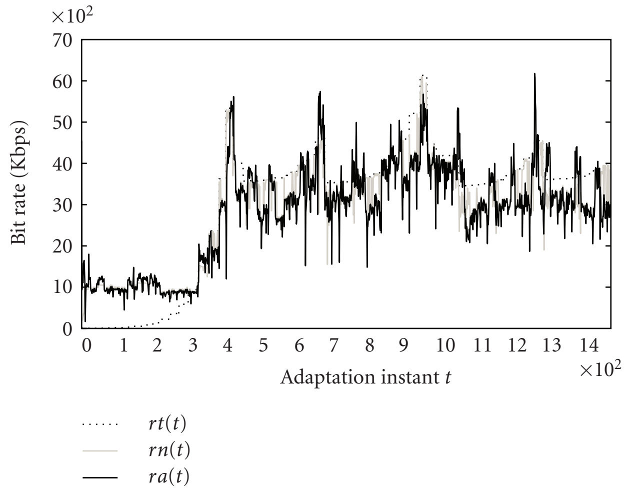

Figure 6: Behavior of $rt(t)$, $rn(t)$ and $ra(t)$ during the transmission.

$\epsilon(rt(t), rn(t))$ is negative (i.e., $rt(t) < rn(t)$) because to $t = [0; 300]$, $rt(t) = 0$. Thus, $rt(t)$ is mapped into L_j such as $rn_j = 200$ Kbps. If the initial allowed bit rate was set at 200 Kbps, then the error in $t = [0; 300]$ would be next to 0. From time $t = 300$ to the end of the transmission the error was 0 or positive. This error behavior shows that $rt(t) \geq rn(t)$. The reason is because, in time t, the actuator selects a QoS level L_k such that rn_k is close (*but never greater*) to the target throughput $rt(t)$ provided by the controller Section 3.1.1. We used this policy since we believe it is better to underestimate the available bandwidth than taking the risk of selecting a QoS level L_k such as $ra_k > rt(t)$, keeping or even increasing losses.

The relationship between rn and ra is also strong, since the correlation coefficient is 0.911 and the P-value is also.0 (the curve rn practically overlaps the curve ra, as showed in Figure 6). The harmonic mean of the errors $\epsilon(rn(t), ra(t))$ is 11.2962 Kbps. This low value indicates that the compression rate (and the bit rate) achieved in the test video matches the reference video compression rate, to a same QoS level

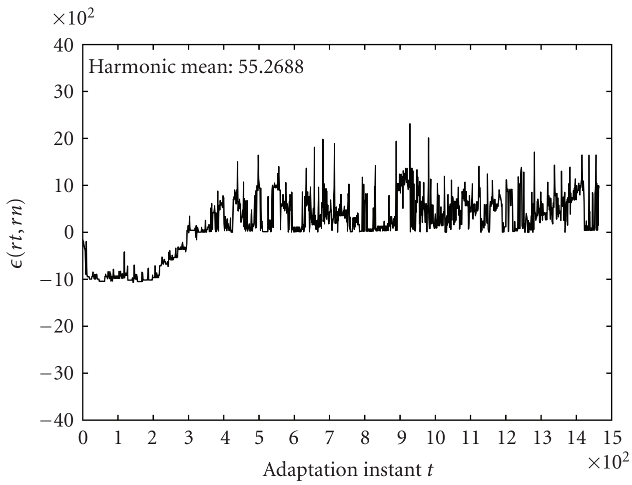

FIGURE 7: Error $\epsilon(rt(t), rn(t))$.

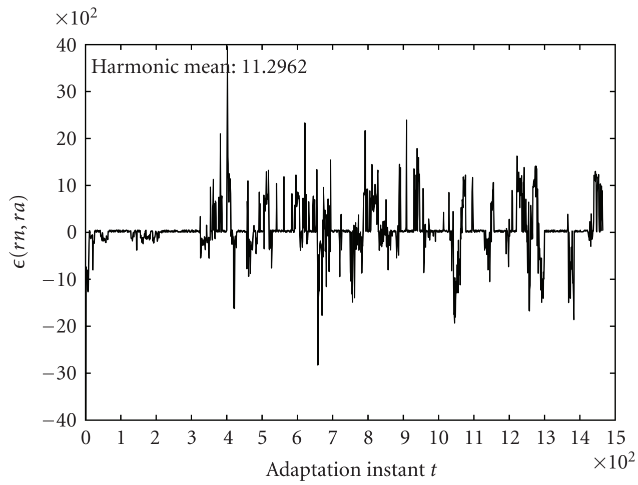

FIGURE 8: Error $\epsilon(rn(t), ra(t))$.

L_k. According to Figure 8, there are some peaks in the error, probably due to the fact that the reference video background is a ballet scene whereas the test video background is a still scenario (see Figures 2 and 4, resp.). The difference between rn and ra decreases during the transmission, due to the $\mathcal{Q}oS_T$ self adjustment mechanism. Figure 9 shows the curve $rt(t)$ and a curve representing the growth of the summed squared errors $\epsilon(rn(t), ra(t))$ ($\text{SSE}\epsilon_{rn,ra}(t)$) during the transmission. In this figure, some breakpoints in the curve $\text{SSE}\epsilon_{rn,ra}(t)$ are highlighted by arrows. These breakpoints are the beginning of ranges where $\text{SSE}\epsilon_{rn,ra}(t)$ grows slowly. Note that these ranges correspond to ranges in the curve $rt(t)$ whose values of the target bit rate are equal or similar. The reason is that the actuator, in a given time t, selects a QoS level L_k such as $rn_k \approx rt(t)$. The achieved bit rate is $ra(t)$ and $\epsilon(rn(t), ra(t)) = k_t$. If in time $t+1$, $rt(t) = rt(t+1)$ (or $rt(t) \approx rt(t+1)$), then the actuator again selects L_k. However, this turn rn_k corresponds to the rate of the rn_k of the test video rather than the reference video, thanks to the $\mathcal{Q}oS_T$ self adjustment mechanism. Therefore, $\epsilon(rn(t+1), ra(t+1)) = k_{t+1} < k_t$.

According to Figure 10, the error $\epsilon(rt(t), ra(t))$ is often greater than $\epsilon(rt(t), rn(t))$ and $\epsilon(rn(t), ra(t))$. This was expected since

$$\epsilon(rt(t), ra(t)) = \epsilon(rt(t), ra(t)) + \epsilon(rn(t), ra(t)). \quad (7)$$

In spite of the harmonic mean of $|\epsilon(rt(t), ra(t))|$ to be more than twice the $\mathcal{Q}oS_T$ granularity (64.261 and 25 Kbps, resp.,), a longer video transmission tends to decrease $\epsilon(rn(t), ra(t))$ and, thus, $\epsilon(rt(t), ra(t))$. In future work, the value 64.261 may be used as a reference to evaluate other strategies for mapping allowed bit rate into application QoS parameters.

Figure 11 also shows the quality (SNR) dynamics during the transmission. This curve is similar to the the $rn(t)$ curve of Figure 6. Therefore, quality really follows bit rate, indicating that the actuator generally selects the QoS level that better fulfills a given target bit rate. Figure 11 also shows the percentage of packets lost between two RR packets. As expected, there are large quality oscillations, since congestion

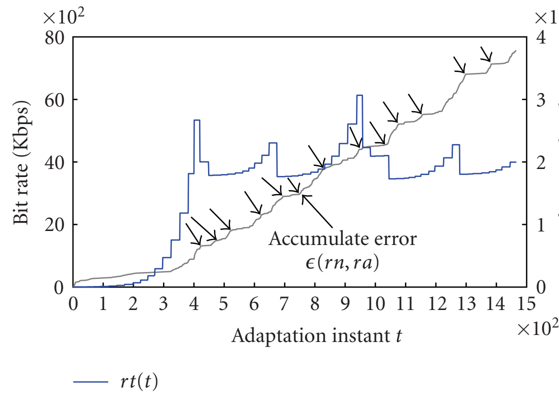

FIGURE 9: Accumulated error $\epsilon(rn(t), ra(t))$.

control schemes (such as LDA+) using an Additive-Increase and Multiplicative-Decrease (AIMD) policy produce abrupt bit rate changes. Larger oscillations especially occur in the presence of losses, when rt is suddenly decreased. Indeed, the AIMD policy is not suitable for multimedia applications such as live video and streaming, where a relatively smooth sending rate is of importance. There are rate control mechanisms—for example, the TCP Friendly Rate Control (TFRC) [15]—more suitable for this kind of applications.

In terms of bit rate adjustment time, Figure 6 shows that curve $rt(t)$ practically overlaps curve $ra(t)$, *indicating* a trivial control/actuation overhead.

Related to the memory usage, Figure 12 shows the $\mathcal{Q}oS_T$ table values $rn_k \times qn_k$. Each point in the graph is a QoS level and they are sorted by rn_k. Note that the relationship between quality and bit rate *is not* monotonicly increasing. This means that in $\mathcal{Q}oS_T$ there are QoS levels L_i and L_j such as

$$rn_i \geq rn_j, \qquad qn_i < qn_j, \quad (8)$$

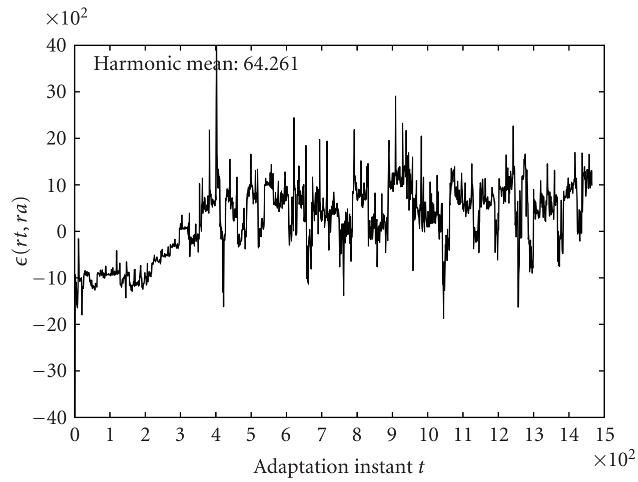

Figure 10: Error $\epsilon(rt(t), ra(t))$.

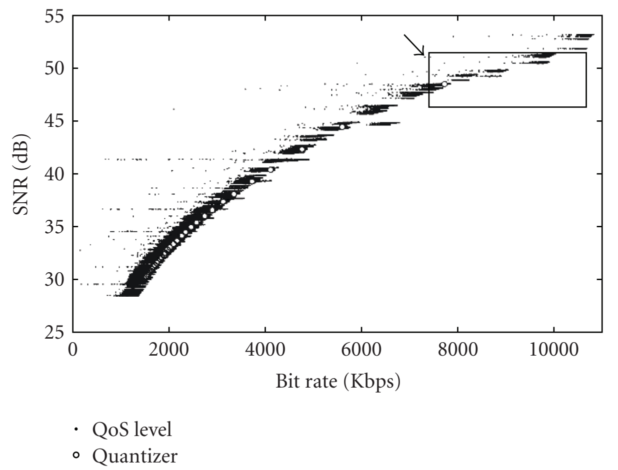

Figure 12: Bit rate × quality.

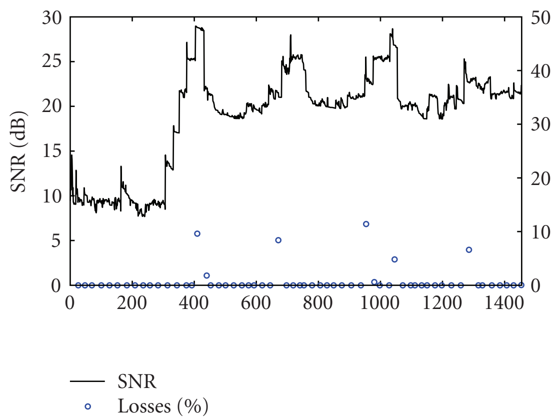

Figure 11: SNR behavior during the video transmission.

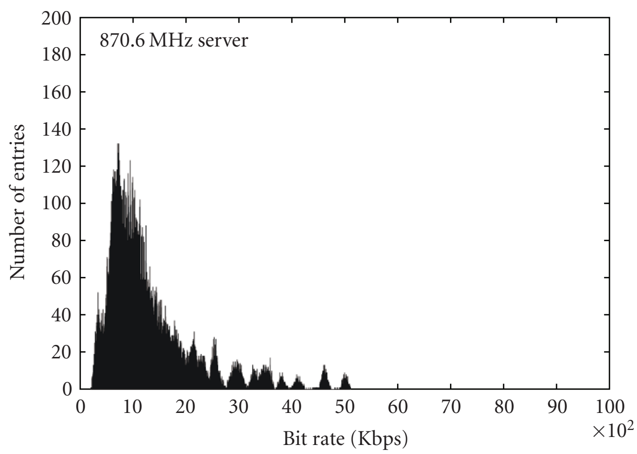

Figure 13: QoS levels distribution per throughput subranges (slow server).

that is, there are QoS levels requiring more bandwidth, but offering an inferior quality than others. Figure 2, for example, shows the same single frame of a stream compressed with two QoS levels L_i and L_j whose entries in $\mathcal{Q}oS_T$ are

$$\begin{gathered}\langle\langle 1,4,62,2,8,2\rangle, 1047.86, 8.96\rangle,\\ \langle\langle 6,6,10,4,8,2\rangle, 1045.09, 21.80\rangle,\end{gathered} \tag{9}$$

respectively. Whereas $rn_i \approx rn_j$, qn_i and qn_j are very different (this is very clear comparing Figure 2(a) and Figure 2(b)). In Figure 12, a set of dispensable QoS levels is gathered in the rectangle. All of them have a quality equal or lower than the QoS level marked by the arrow but requiring more bandwidth.

Moreover, it is widely accepted the limit of 20 db as a minimum of SNR for a picture to be viewable. Then, we could also discard QoS levels L_k such as $qn_k < 20$. (The resultant clip is available at http://www.youtube.com/watch?v=rw7V7U7qDN0 for the reader to draw own conclusions about the end-quality.) Alternatively, we could calculate the minimum transmission bit-rate for a minimum required picture quality based on the Rate Distortion theory [16]. The minimum quality should be preferentially obtained from subjective tests, despite the controversial about the accuracy of these tests (see Section 3.3). Levels bellow the minimum quality can be discarded.

Figure 12 also shows $qtz \times rn_k$. Note that a bit rate adjustment based only on the quantizer adjustment (a very common approach) cannot smoothly change the bit rate.

Finally, in order to investigate the influence of processing power on the QoS levels distribution among the throughput subranges, we also generated the $\mathcal{Q}oS_T$ table in a slow server, a Intel Pentium III 870.639 MHz processor. Figure 13 shows a histogram representing the QoS levels distribution of $\mathcal{Q}oS_T$ for this server. QoS levels are predominantly concentrated between 1500 and 3000 Kbps. The highest throughput is around 5000 Kbps. Note that the QoS levels tend to concentrate on the highest throughput improving the server processing power and vice-versa. Hence, the throughput subrange where a QoS level is placed depends on the server processing power used to generate $\mathcal{Q}oS_T$.

To summarize, the above results indicate that: (1) $\mathcal{Q}oS_T$ provides a large and continuous range of possible throughputs. This is a necessary condition for testing the quality provided by a rate controller; (2) initial values rn_k (nominal rate) and qn_k (nominal quality) of the QoS level L_k in $\mathcal{Q}oS_T$, obtained from the reference video, are a reasonable approximation of the values $ra(t)$ and $qa(t)$, the actual bit rate and quality achieved for the test video when the encoder is set to L_k; (3) the minimum and maximum bit rate $[m, M]$ bounded by the tool depend on the server processing power. A powerful video server increases both values; (4) quality oscillation occurs due to the rate controller approach used to compute the allowed (target) bit rate. The test tool only tries to reach this target bit rate. If the target bit rate oscillates or/and changes suddenly, then the quality will also oscillate or/and change suddenly; and (5) thousands of QoS levels may be discarded, reducing the tool memory needs.

5. Related Work

Cranley et al. [10] have proposed an optimal way in which multimedia transmissions should be adapted in response to network conditions to maximize the user-perceived quality. Similar to our work, their approach assumes that within the set of different ways to achieve a target bit rate, there exists an encoding maximizing the user-perceived quality. Extensive subjective tests suggests that an Optimal Adaptation Trajectory (OAT) in the space of possible encoding does exist and that it is related to the content type. In their paper, the authors explore the possibility of applying objective metrics to discover the OAT and compare it to those found through extensive subjective tests.

Differently from the work of Cranley et al., our work is not supposed to be a model or architecture for QoS adaptation, but simply a tool for testing and comparing rate controllers. Therefore, it is a support for the research in this area. However, the OAT function could be used in our tool as a degradation path rather than the $\mathcal{Q}oS$ function.

Yan et al. presents in [17] a media- and TCP-friendly rate-based congestion control algorithm (MTFRCC) for scalable video streaming on the Internet. To each transmission at rate $r_s \in [m_s, M_s]$ of a sender s is associated a utility function $U_s(r_s)$. They assume that U_s is twice continuously differentiable in $[m_s, M_s]$. The objective of the algorithm is to choose source rates r_s such that the overall utility is maximized, that is, to optimize the video quality of all streams. It should be noted that the utility function varies according to video coding scheme used. To tailor the utility function to application quality, Yan et al. use the rate-distortion function such as

$$U_s(r_s) = -D_s(r_s), \tag{10}$$

where $D_s(r_s)$ is the rate-distortion function for finer grain scalable (FGS) video derived from a mixture-Laplacian statistical model of FGS video streams proposed in [18] and given by:

$$D_s(r_s) = 2^{\rho_1 \cdot r_s + \rho_2 \sqrt{r_s} + \rho_3,} \tag{11}$$

where ρ_1, ρ_2, and ρ_3 are parameters to be empirically evaluated. They stand for the streaming rate and for the distortion of a single frame. The values of ρ_1, ρ_2, and ρ_3 vary depending on the source video stream. With the available $r_s - D$ information, the values of ρ_1, ρ_2, and ρ_3 can be computed during the encoding process, for real-time operation. The values are computed once for each video sequence and it is assumed that they remain constant throughout the entire streaming process. The rate-distortion function in (11) is strictly decreasing and convex whereas the utility function in (10) is strictly increasing and concave. In practice, the rate r_s has to be, in the congestion avoidance phase, not smaller than the bit rate of the base layer m_s; otherwise the application quality will be significantly harmed and packet delivery will be unacceptably delayed.

The $\mathcal{Q}oS$ function is similar to the U_s function, in terms of purpose and construction. However, in practice, the cost of determination of the $\mathcal{Q}oS$ to each QoS level L_k is very high depending on the encoder parameters compounding L_k; we again highlight that this process is executed once and the $\mathcal{Q}oS$ can be used for different video transmissions. On the other hand, $\mathcal{Q}oS$ is not bounded to three parameters and can be more continuous than U_s. Moreover, $\mathcal{Q}oS$ is tailored to the video during the transmission, that is, the quality and bit rate associated to the QoS levels do not remain constant throughout the entire video delivery process.

Ke et al. present in [5], a simulation tool integrating the EvalVid tool-set [19] and NS-2. EvalVid is a tool-set for evaluating video quality transmitted over a real or simulated communication network. The EvalVid's purpose is to assist researchers in evaluating their network mechanisms or designed protocols in terms of user-perceived video quality over a real or simulated network. To improve the simulation model, Ke et al. enhanced some interfaces into EvalVid. With the enhancement, the tool-set enables not only network-related researchers to evaluate real video streams on their proposed network designs or protocols, but also video-related researchers to evaluate video quality of their designed video coding mechanisms using a more realistic network. On the one hand, the work is not bounded by testing rate controllers and permits tests without a real environment and controller implementation. On the other hand, the tool set uses encoded video trace files generated from YUV files. This aspect became hard to test controllers based on setting the encoder parameters in real-time.

Lotfallah et al. propose in [20] a framework for advanced video traces which enables the evaluation of video transmission over lossy packet networks, without requiring the actual videos. The two main components of this framework are (1) advanced video traces which combine the conventional video traces with a parsimonious set of visual content descriptors, and (2) quality prediction schemes that based on the visual content descriptors provide an accurate prediction of the quality of the reconstructed video after lossy network transport. The video traces represent a small number of encodings (versions) with different encoding bit rates for each video sequence and estimates the reconstructed quality using the motion activity levels of the underlying visual content (or, in general, any content descriptor(s) that highly correlate with the reconstructed quality). The number of provided QoS levels is bounded by the number of versions, whereas in our work this number is given by the number and the nature of the QoS parameters used.

6. Conclusions and Future Work

In this paper, we described a live video delivery tool that can be used to test RTP-based rate controllers providing complementary results to those ones achieved by simulation. Particularly, it is useful to provide results related to actual achieved quality, overhead introduced by the control, and actual throughput. The tool may aid rate controller designers to test their strategies regarding performance aspects hard to evaluate by simulation (e.g., control overhead, frame rate at the clients, quality achieved, quality oscillation, etc.). Since it is highly modular, the tool can use any controller structured as a black box whose inputs are round trip delay and loss rate and the output is the target throughput.

Our results indicate that (1) the actuator often finds a nominal throughput *close to* the target throughput; (2) the self adjustment mechanism of $\mathcal{Q}oS_T$ satisfactorily corrects the throughput and quality nominal values of the QoS levels used for rate adapting during the video transmission (note that these values are strongly related to the reference video in the beginning of the transmission); and (3) the encoding/control overhead is not critical in the end-to-end delay when the server answers a single video request.

Even though our tool has been designed and implemented to be a tool for RTP-based controller test support, its actuation strategy can be exploited as part of a rate control mechanism of live video delivery tools. Note that it was not our intent to build a fully functional live video application since there are many libraries supporting the development of such applications and even fully functional open source applications. However, to provide support for different encoders, many of them have a large and complex source code. In addition, some of them generate only CBR streams. Therefore, our tool can be used to test and compare different control approaches prior to the construction of a live video delivery application with rate control.

Some limitations of the current version of our tool include: use of pre-stored raw video rather than real-time captured video, absence of client-side buffering for smoothing jitter, and MPEG-2 encoding rather than H.264/AVC, which delivers similar quality at lower data rates. However, a future work includes to replace the MPEG-2 encoder by the H.264/AVC Scalable Video Coding (SVC) to define QoS levels in terms of the multi-dimensional scalability provided by this encoder [21] (previous work on rate control for H.264/AVC/SVC streams was primarily based on changing resolution layers by using the FGS feature. However, FGS—include in a draft document—has been removed according to [22].). The use of a VBR H.264/AVC/SVC encoder performing transmission over an RTP stack rather than the current MPEG-2 would request minor modifications. More precisely, it would be necessary: (1) to identify in the source code the variables used for the encoder settings and select those ones to compound QoS levels; (2) to allocate them as shared memory assuring mutual exclusion (since the actuator runs concurrently with the encoder); and (3) to identify the relationship of these variables with others and the encoder data structures, especially for variables related to the temporal compression (this is the hardest part!). A currently practical difficulty in using H.264/AVC is the time demanded by this encoder to compress a video in real-time, when the server is a common PC. We performed some tests on a two processors Intel Pentium CPU 2.80 GHz machine using the JM version 15.0 H.264/AVC encoder implementation (http://iphome.hhi.de/suehring/tml/). The frame rate of encoding a raw video (QCIF format, 30 fps, and baseline profile), for example, was less than 1 fps. Nevertheless, we believe presently common PC's will provide enough processing power to encode live video in the H.264/AVC standard by software.

Another future work is to test and compare the performance of more recent TCP-friendly rate control mechanisms using our tool, such as TFRC [15].

Currently, we are designing a new version of the tool based on the Datagram Congestion Control Protocol (DCCP) rather than RTP over UDP. By using this new version, we will be able to verify the actual video quality provided by different congestion control mechanisms, such as CCID 2 (Congestion Control ID 2), CCID 3, and CCID 4, when used to transport both streaming applications data as live video data applications.

The resultant video received by the client in the tests can be viewed at http://www.youtube.com/watch?v=rw7V7U7qDN0. By watching this video, the reader can draw own conclusions about the quality variation.

References

[1] J.-Y. L. Boudec, "Rate Adaptation, Congestion Control and Fairness: a Tutorial," 2008.

[2] C. Koliver, K. Nahrstedt, J.-M. Farines, J. D. S. Fraga, and S. A. Sandri, "Specification, mapping and control for QoS adaptation," *Real-Time Systems*, vol. 23, no. 1-2, pp. 143–174, 2002.

[3] S. Lee and K. Chung, "TCP-friendly rate control scheme based on RTP," in *Proceedings of the International Conference on Information Networking (ICOIN '06)*, I. Chong and K. Kawahara, Eds., vol. 3961 of *Lecture Notes in Computer Science*, pp. 660–669, Springer, Sendai, Japan, 2006.

[4] K. Pawlikowski, "Do not trust all simulation studies of telecommunication networks," in *Proceedings of the International Conference on Information Networking (ICOIN '03)*, vol. 2662, pp. 3–12, Jeju Island, Korea, 2003.

[5] C.-H. Ke, C.-H. Lin, C.-K. Shieh, and W.-S. Hwang, "A novel realistic simulation tool for video transmission over wireless network," in *Proceedings of the IEEE International Conference on Sensor Networks, Ubiquitous, and Trustworthy Computing*, pp. 275–281, Los Alamitos, Calif, USA, June 2006.

[6] S. Fischer, A. Hafid, G. V. Bochmann, and H. de Meer, "Cooperative QoS management for multimedia applications," in *Proceedings of the 4th IEEE International Conference on Multimedia Computing and Systems (ICMCS '97)*, pp. 303–310, IEEE Press, Ottawa, Canada, June 1997.

[7] M. Fry, A. Seneviratne, and V. Witana, “Delivering QoS controlled continuous media on the World Wide,” in *Proceedings of 4th IFIP International Workshop on Quality of Service (IWQoS ’96)*, Paris, France, 1996.

[8] G. Ghinea and J. P. Thomas, “Improving perceptual multimedia quality with an adaptable communication protocol,” *Journal of Computing and Information Technology*, vol. 13, no. 2, pp. 149–161, 2005.

[9] A. Rodriguez, A. Gonzalez, and M. P. Malumbres, “Hierarchical parallelization of an H.264/AVC video encoder,” in *Proceedings of the IEEE International Symposium on Parallel Computing in Electrical Engineering (PARELEC ’06)*, pp. 363–368, IEEE Computer Society, Los Alamitos, Calif, USA, 2006.

[10] N. Cranley, P. Perry, and L. Murphy, “User perception of adapting video quality,” *International Journal of Human Computer Studies*, vol. 64, no. 8, pp. 637–647, 2006.

[11] O. Nemethova, M. Ries, E. Siffel, and M. Rupp, “Quality assessment for H.264 coded low-rate and low-resolution video sequences,” in *Proceedings of the 3rd IASTED International Conference on Communications, Internet, and Information Technology (CIIT ’04)*, pp. 136–140, St. Thomas, Va, USA, November 2004.

[12] A. Watson and M. A. Sasse, “Measuring perceived quality of speech and video in multimedia conferencing applications,” in *Proceedings of the 6th ACM International Conference on Multimedia*, pp. 55–60, Bristol, UK, September 1998.

[13] ITU-T Recommendation J.149, “Method for specifying accuracy and crosscalibration of video quality metrics (VQM),” 2004.

[14] D. Sisalem and A. Wolisz, “LDA+: a TCP-friendly adaptation scheme for multimedia communication,” in *Proceedings of the IEEE International Conference on Multi-Media and Expo (ICME ’00)*, pp. 1619–1622, IEEE Press, New York, NY, USA, July-August 2000.

[15] S. Floyd, M. Handley, J. Padhye, and J. Widmer, “TCP Friendly Rate Control (TFRC): Protocol Specification,” RFC 5348 (Proposed Standard), September 2008.

[16] L. D. Davisson, “Rate-distortion theory and application,” *Proceedings of the IEEE*, vol. 60, no. 7, pp. 800–808, 1972.

[17] J. Yan, K. Katrinis, M. May, and B. Plattner, “Media- and TCP-friendly congestion control for scalable video streams,” *IEEE Transactions on Multimedia*, vol. 8, no. 2, pp. 196–206, 2006.

[18] M. Dai, D. Loguinov, and H. Radha, “Rate-distortion modeling of scalable video coders,” in *Proceedings of the International Conference on Image Processing (ICIP ’04)*, vol. 5, pp. 1093–1096, Society Press, October 2004.

[19] J. Klaue, B. Rathke, and A. Wolisz, “EvalVid—a framework for video transmission and quality evaluation,” in *Proceedings of the 13th International Conference on Modelling Techniques and Tools for Computer Performance Evaluation*, pp. 255–272, Urbana, Ill, USA, 2003.

[20] O. A. Lotfallah, M. Reisslein, and S. Panchanathan, “A framework for advanced video traces: evaluating visual quality for video transmission over lossy networks,” *EURASIP Journal on Applied Signal Processing*, vol. 2006, Article ID 42083, 21 pages, 2006.

[21] P. Ni, A. Eichhorn, C. Griwodz, and P. Halvorsen, “Fine-grained scalable streaming from coarse-grained videos,” in *Proceedings of the 18th International Workshop on Network and Operating System Support for Digital Audio and Video (NOSSDAV ’09)*, pp. 103–108, Williamsburg, Va, USA, June 2009.

[22] ITU-T Recommendation H.264 H.264, “Advanced video coding for generic audiovisual services,” November 2007.